A critical role for IRF5 in regulating allergic airway inflammation

Adam J. Byrne[1,2], **Miriam Weiss**[1], **Sara A. Mathie**[2], **Simone A. Walker**[2], **Hayley L. Eames**[1], **David Saliba**[1], **Clare M. Lloyd**[2,*], and **Irina A. Udalova**[1,*]

[1]Kennedy Institute of Rheumatology, University of Oxford, U.K

[2]Inflammation, Repair & Development Section, National Heart & Lung Institute, Imperial College London, UK

Abstract

Interferon regulatory factor 5 (IRF5) is a key transcription factor involved in the control of the expression of pro-inflammatory cytokine and responses to infection, however its role in regulating pulmonary immune responses to allergen is unknown. We used genetic ablation, adenoviral vector-driven overexpression and adoptive transfer approaches to interrogate the role of IRF5 in pulmonary immunity and during challenge with the aero-allergen, house dust mite. Global IRF5 deficiency resulted in impaired lung function and extracellular matrix (ECM) deposition. IRF5 was also essential for effective responses to inhaled allergen, controlling airway hyper-responsiveness, mucus secretion and eosinophilic inflammation. Adoptive transfer of IRF5-deficient alveolar macrophages into the WT pulmonary milieu was sufficient to drive airway hyper-reactivity, at baseline or following antigen challenge. These data identify IRF5-expressing macrophages as a key component of the immune defence of the airways. Manipulation of IRF5 activity in the lung could therefore be a viable strategy for the redirection of pulmonary immune responses and thus, the treatment of lung disorders.

Introduction

Asthma is a heterogeneous disease of the airways characterized by airway remodelling, mucus production, airway hyperresponsiveness (AHR), and inflammation. Although asthma has traditionally considered to be a Th2-driven disease, many T-cell directed therapies have not been effective in clinical trials[1,2]. The lack of effective therapies for some types of asthma might reflect the poor understanding of the specific immunological pathways that lead to the disease. Interferon regulatory factor 5 (IRF5) is a key transcription factor involved in the control of the expression of pro-inflammatory cytokine responses to

Corresponding authors: Adam J Byrne: Inflammation, Repair & Development Section, National Heart and Lung Institute, Sir Alexander Fleming Building, Faculty of Medicine, Imperial College, South Kensington, London SW7 2AZ, UK. abyrne@imperial.ac.uk; Tel: +44 (0)2075945016; Fax: +44 (0)2075943119. Irina A. Udalova: Kennedy Institute of Rheumatology, University of Oxford, Roosevelt Drive, Oxford, OX3 7FY, U.K. irina.udalova@kennedy.ox.ac.uk; Tel: +44 (0)1865612600; Fax: +44 (0)1865612601. Clare M. Lloyd: Inflammation, Repair & Development Section, National Heart and Lung Institute, Sir Alexander Fleming Building, Faculty of Medicine, Imperial College, South Kensington, London SW7 2AZ, UK. c.lloyd@imperial.ac.uk; Tel: +44 (0)2075943102; Fax: +44 (0)2075943119.

microbial infection and type I interferon responses to viral infection 3. IRF5 mRNA expression is increased in response to IFN-g and GM-CSF 4, whereas activation of IRF5 protein occurs in response to immune signaling pathways, such as downstream of TLRs etc, via post-translational modifications such as phosphorylation and ubiquitination 5. Polymorphisms in the gene encoding IRF5 that lead to higher mRNA expression are associated with many autoimmune diseases, such as rheumatoid arthritis6, Sjogrens syndrome7, systemic lupus erythematosus8, multiple sclerosis7 and inflammatory bowel disease9. Emerging genetic studies have provided evidence that implicates IRF5 in the pathogenesis of allergic disease. Wang *et al* identified a common IRF5 haplotype to be associated with asthma and the severity of asthmatic symptoms and furthermore, the risk associated with IRF5 was found to be opposite in direction to those for autoimmune disorders 10. Recently, we demonstrated that IRF5 is critical in establishing inflammatory macrophage phenotypes involved in the positive regulation of Th1/Th17 associated mediators, such as IL-1, IL12β, IL-23 and TNFα and the negative regulation of Th2 associated-mediators, such as IL-10 3,4.

Macrophages are the most abundant immune-cell type present in the lung environment under homeostatic conditions and are therefore strategically positioned to control the innate defense of the airways 11,12. Two defined populations of macrophages in the lung are characterized by unique properties and functions 13. Alveolar macrophages (AMs) exist in in the airway lumen and are characterized by high expression of CD11c but lack CD11b expression 14. Interstitial macrophages (IMs) reside in the lung parenchyma, express high levels of CD11b, low levels of CD11c and have been shown to control endotoxin-induced airway inflammation 15. As a critical component of pulmonary immunity, alveolar macrophages are tightly regulated in order to preserve homeostasis; however, the molecular mechanisms by which this occurs are not well understood.

We find that macrophages are the predominant IRF5-expressing cell type in the pulmonary compartment under homeostatic conditions. The absence of IRF5 during exposure to the clinically relevant allergen, house dust mite (HDM), resulted in increased airway hyper-responsiveness and allergic inflammation, concomitant with elevated expression of extracellular matrix molecules and collagen deposition. Significantly, adoptive transfer of IRF5-deficient alveolar macrophages into the WT milieu was sufficient to drive airway hyper-reactivity, even in the absence of antigen stimulation. Conversely, over-expression of IRF5 resulted in ablated AHR, diminished eosinophilia and decreased type-2 cytokine production. These data identify IRF5-expressing macrophages as a key component of the immune defence of the airways. Manipulation of IRF5 activity in the lung could thereby be a viable strategy for the redirection of pulmonary immune responses and thus, the treatment of lung disorders.

Results

IRF5 deficiency leads to augmented Type 2 responses in the lung after HDM exposure

In order to determine the role of IRF5 in regulating the pulmonary environment, we first exposed mice to the aeroallergen, house dust mite (HDM), instilled directly into the airways (Fig. 1A). Ablation of IRF5 had a profound effect on airway function, since IRF5$^{-/-}$ mice

were hyper-responsive to inhaled methacholine challenge, showing increased airway resistance following three weeks of HDM exposure (Fig. 1B and 1C). PBS treated IRF5^{-/-} mice displayed increased airway resistance in comparison to wild-type (WT) controls even in the absence of allergen stimulation (Fig. 1B and C). Examination of cellular inflammation revealed that total cellular infiltrate and eosinophila were enhanced in the BAL (Fig. 1D), but not lung (Fig. 1E), of IRF5 deficient mice; analysis of H&E stained lung sections confirmed these observations (Fig. 1F). Furthermore, IL-13 secretion into the airspaces (Fig. 1G) and lung eotaxin-2 levels (Fig. 1H) were enhanced in IRF5-deficient animals after week 3 of allergen exposure; as were expression levels of IL-4, 5, 13 and eotaxin-2 (Supplemental Fig. 1A). Moreover, alveolar macrophages in the BAL of PBS treated IRF5-/- mice displayed higher intracellular level of IL-13, in comparison to WT controls (Supplemental Fig 1B) even in the absence of IL-13 secretion in the BAL (Fig 1G), implying a direct effect of IRF5 on inflammatory response in AMs. In addition, there was a significant increase in the population of IL-13^{+} CD4^{+} T-lymphocytes (Fig. 1I). However, there was no difference in total Th1, Th17 and total innate lymphoid (ILC) populations (Supplemental Fig. 1C), or in IL-13^{+} producing ILC2 cells (Supplemental Fig. 1D). Interestingly, we detected a small number of IL-17^{+} producing ILC3 cells in the lung of WT animals and this population was reduced to baseline levels in the IRF5^{-/-} mice (Supplemental Fig. 1D). Although ILC3 populations have been shown to be important for obesity associated deteriorations in lung function16, their absence in this model, did not result in a reduction in airway hyper-responsiveness. We also observed augmented levels of HDM-specific IgE (Supplemental Fig. 1E), no change in HDM-IgG1 (Supplemental Fig. 1F) responses and decreased levels of HDM-IgG2a in IRF5^{-/-} mice (Supplemental Fig. 1G); these humoral responses are consistent with previously reported findings 17,18. Taken together, all classical indicators of allergic immune responses were exacerbated in HDM exposed IRF5-deficient mice concomitant with airway inflammation and AHR.

Pulmonary IRF5 controls airway remodeling

Since type-2 responses were enhanced in IRF5 deficient mice in comparison to WT controls (Fig. 1), we next examined whether these changes resulted in alterations in mucus secretion and airway remodeling. Goblet cell hyperplasia was increased in HDM-treated IRF5^{-/-} mice in comparison to WT controls (Fig. 2A and C). Muc5b, but not Muc5ac was significantly elevated after allergen exposure (Supplemental Fig. 2A, B). Interestingly, a recent study by Roy *et al* demonstrated that murine Muc5b, but not Muc5ac is required for mucociliary clearance and for maintaining homeostasis in the murine lung 19. Moreover, IRF5^{-/-} mice exhibited increased extracellular matrix (ECM) deposition around the airways, in comparison to WT controls, as indicated by Sirius red staining (Fig. 2 B, D and E). These alterations were also accompanied by an enhanced M2 (Supplementary Fig. 2C, D) and a reduced M1 (Supplementary Figure 2E) signature in the lung. These data indicate that IRF5 deficiency leads to enhanced ECM deposition and thus, normal airway function and homeostasis is disrupted. Therefore our data demonstrate a novel role for IRF5 in regulating airway function via enhanced Type 2 skewing (Fig. 1), in addition to mucus and collagen production in response to HDM (Fig. 2).

IRF5 deficiency impairs pulmonary homeostasis via increased extracellular matrix deposition and IL-13 production

We have previously demonstrated that IRF5 expression is a key determinant of inflammatory macrophage phenotype 4; Macrophages are the predominant IRF5-expressing cell type in the pulmonary compartment under homeostatic conditions (Fig 3A). IRF5 appeared to be expressed in alveolar epithelium (Supplementary Fig 3B), however, by analyzing cells obtained from bronchoalveolar lavage we found that the IRF5 expressing cells in the airway lumen, the optimum position to influence airway function, were almost exclusively AMs (Fig. 3B and Supplementary Fig 3A, B). As IRF5-expressing AMs were the predominant IRF5 expressing cell present in the airway lumen, and the role of pulmonary macrophage sub-types in maintenance of airway function is unknown, we next investigated whether adoptive transfer of IRF5^{-/-} alveolar macrophages into the WT airway could reproduce the phenotype we observed in IRF5^{-/-} mice. Adoptive transfer of WT or IRF5^{-/-} macrophages directly to the lungs of WT mice (Fig. 3C), did not result in a pulmonary inflammatory infiltrate within the timescale tested (Fig 3D, E); donor cells could be recovered from the airway lumen 24h after transfer (Supplementary Fig 3C). However, transfer of IRF5^{-/-} alveolar macrophages into a WT lung environment resulted in a significant alteration in normal airway resistance (Fig. 3F). These changes were accompanied by an increase in levels of IL-13 in the airway lumen as determined by ELISA (Fig. 3G) and the expression of collagen-1α1 (Fig. 3H) and fibronectin (Fig. 3I) in whole lung tissue homogenates. In order to further investigate whether the observed changes in airway resistance were due to macrophage driven IL-13 production, we prophylactically treated WT mice with either an IL-13 blocking antibody, or isotype control, prior to adoptive transfer of IRF5^{-/-} AMs (Fig. 3J). Consistent with our previous observations, blockade of IL-13 was sufficient to ameliorate IRF5^{-/-} macrophage driven lung function changes, in comparison to isotype control treated mice (Fig 3K). Thus, delivery of IRF5-deficient alveolar macrophages is sufficient to influence the pulmonary environment and recapitulate, in a WT lung, the pathophysiological changes observed in IRF5^{-/-} mice in an IL-13-dependent manner.

IRF5-expressing AMs control responses to inhaled aeroallegen

As the key features of allergic airways disease were exacerbated in HDM exposed IRF5-deficient mice in comparison to controls (Fig. 1 and 2) and IRF5-expressing AMs were capable of controlling lung homeostasis (Fig. 3), we next examined whether IRF5-expressing AMs were involved in responses to inhaled aeroallergen. To achieve this, we adoptively transferred WT or IRF5^{-/-} macrophages directly to the lungs of WT mice followed by HDM administration (Fig. 4A). HDM exposed IRF5^{-/-}-AM recipients, had heightened airway hyperreactivity to methacholine (Figure 4B), as well as increased cellular inflammation in the BAL (Figure 4C) and lung (Figure 4D), increased BAL eosinophilia (Figure 4E), increased lung IL-4 levels (Supplementary Figure 4A) and augmented IL-13 levels in both the BAL (Figure 4F) and lung (Figure 4G) in comparison to WT-AM, HDM exposed recipients. These data indicate that IRF5-expressing alveolar macrophages regulate responses to inhaled aeroallergen via Th2 cytokines, in particular IL-13.

Overexpression of IRF5 ameliorates house dust mite-mediated airway hyperresponsiveness

Having shown that IRF5 deficiency resulted in dramatic effects on pulmonary immunity both basally and during allergen exposure, we next sought to determine the effect of overexpression of IRF5 in the airway lumen. First, we determined an appropriate intranasal dose of an adenoviral vector expressing IRF5 (AdIRF5), or empty vector (AdC), which would induce augmented IRF5 expression in the lungs (Supplemental Fig. 5A, B) without producing an associated inflammatory response (Supplemental Fig. 5C-F). Moreover, we observed no changes in cellular influx in the BAL of mice administered with the IRF5 encoding vector compared with the control vector (Supplemental Fig. 5G). Next, we used this optimized dosing regimen to generate mice over-expressing pulmonary IRF5 and then exposed them to HDM extract intra-nasally (Fig. 5A). Two days after instillation with AdIRF5, alveolar macrophages expressed human IRF5 whereas IMs did not appear to take up the virus at this time-point (Supplemental Fig. 5H), consistent with previously observed rapid internalization of adenovirus by AMs 20. After 3 weeks of allergen exposure, we observed amelioration of airway hyper-reactivity in mice exposed to AdIRF5, in comparison to mice treated with AdC (Fig. 5B and C). Cell infiltration in the airway lumen was unaffected by IRF5 overexpression (Fig. 4D). The observed changes in lung function in AdIRF5 mice were accompanied by reduced recruitment of eosinophils to the airway tissue (Fig. 5E). Interestingly, in the IRF5$^{-/-}$ model we see these cellular changes in the BAL rather than the lung tissue (Figure 1D and E). This discrepancy in cellular trafficking is likely due to differences in models or systems (transient overexpression two day before challenge versus global deficiency). Moreover, H&E staining revealed reduced inflammation around the airways in AdIRF5 treated mice (Fig. 5F and G) in addition diminished levels of type-2 chemokines and cytokines, such as and IL-13 (Fig. 5H) eotaxin-2 (Fig. 5I).

Overexpression of IRF5 results in ameliorated airway remodeling after HDM treatment

Goblet cell hyperplasia was significantly diminished in IRF5-overexpressing mice, as determined by PAS staining and mucus scoring (Fig. 6A, C); however, airway remodeling was not affected by IRF5 overexpression at the time-point investigated (Fig. 6B, D). These data indicated that over-expression of IRF5 results in an enhanced ability to regulate immune responses in the lung following allergen exposure, since augmented expression of IRF5 resulted in ablated AHR, diminished the production of type-2 cytokines and decreased eosinophilia after HDM challenge. A complex network of immune pathways regulate the lung environment and disruption of this system by inhaled particles leads to a break in homeostasis; our data indicate that IRF5-expressing macrophages play a central role in the regulation of these responses.

Discussion

A key function of the pulmonary tract is the ability to maintain immune homeostasis despite continuous exposure to inhaled antigens. Although macrophages are ideally placed to contribute to the fine-tuning of the pulmonary immune system, the mechanism by which this is achieved is thus far unknown. This work defines a previously undescribed immune pathway by which IRF5-expressing macrophages can directly regulate the lung

environment. IRF5 expression in alveolar macrophages controls pulmonary function since deletion of IRF5 leads to the establishment of a fibrotic phenotype, without affecting levels of TGF-β or IL-10 expression in the lung (Fig 2. and Supplementary Fig. 5). Adoptive transfer of IRF5-deficient alveolar macrophages into a WT environment is sufficient to induce AHR and airway remodeling leading to IL-13 secretion under steady state conditions (Fig. 3). Of interest, several laboratories have described IL-13 producing macrophages in the context of COPD 4,21, fibrotic disease 22–24, RSV infection 19,21,25, after particle inhalation 26 or in response to IL-25 or IL-33 27. Interestingly, a recent report by Saigusa *et al* 32 described a role for IRF5 as a positive regulator of key genes involved in fibrosis in dermal fibroblasts at steady state and after bleomycin challenge 26. Dalmas *et al*33 found IRF5 to be negatively associated with collagen deposition and remodeling in adipose tissue 27. Together, these studies indicate that IRF5 plays a role in driving fibrotic processes, but these roles maybe pleiotropic depending on the tissue and context.

IRF5 is a key component of interferon (IFN) signaling and there is evidence to suggest that the type-1 IFN system is involved in pathogenesis of Th2 disease, as reduced IFN-signatures have been observed in asthma patients in comparison to controls 26–28. Interestingly, our work shows that IRF5 appears to control aspects of allergic airways disease, as IRF5 overexpression appears to shift the inflammatory profile in the lung from eosinophilic inflammation, towards a neutrophilic signature. Recently, we demonstrated that IRF5 is critical in establishing inflammatory macrophage phenotypes involved in the positive regulation of Th1/Th17 associated mediators and the negative regulation of Th2 associated-mediators, such as IL-10 3,4. Interestingly, in models of lupus and obesity, respectively, IRF5-deficient mice were associated with increased expression of Type 2 cytokines 18. Recently, Wang *et al* identified a common IRF5 haplotype to be associated with asthma and the severity of asthmatic symptoms and furthermore, the risk associated with IRF5 was found to be opposite in direction to those for autoimmune disorders 10; our data provide mechanistic evidence to support these findings. Our previous data have demonstrated a critical role for IRF5 in defining the M1 lineage, based on largely *in vitro* systems. *In vivo*, macrophages are highly plastic and during pulmonary inflammatory disease, macrophage populations are capable of finely tuning their activity and develop mixed phenotypes 28–30. Our data here indicate that although pulmonary macrophages express M2 markers, they also express IRF5 and are thus primed to adapt to various environmental signals.

In summary, this work defines a novel pathway by which alterations in IRF5 expression resulted in the development of AHR. We outline a vital role for IRF5 in mediating pulmonary immunity and dictating allergic immune responses in the lung. The novel relationships between IRF5, lung immunity and AHR reported here have the potential to impact therapies for asthma and highlight IRF5 as a molecular target for the treatment of pulmonary disease.

Materials and Methods

Animals

Female WT or IRF5^{-/-} mice on a C57BL/6 background, 6-8 weeks old, received 25 μg HDM extract (*Dermatophagoides pteronyssinus* in phosphate-buffered saline, PBS, Greer

Laboratories, Lenoir, NC) or 25 μl PBS intra-nasally, 5 days a week for the indicated durations. UK Home Office guidelines for animal welfare based on the Animals (scientific procedures) act 1986 were strictly observed. The Imperial College London Animal Welfare and Ethical Review Body (AWERB) approved this protocol. All surgery was performed under ketamine and sodium pentobarbital anesthesia and all efforts were made to minimize suffering.

Measurement of AHR

Airway responsiveness was determined by direct measurements of resistance (RI) and compliance (Cdyn) in anesthetized and tracheotomised mice in response to inhaled PBS or methacholine (MCh; Sigma, Cambridge, UK), at the indicated doses, for 1 minute in an EMMS system (EMMS, Hampshire, UK).

Cell preparations

In order to obtain BAL, the airways of the mice were lavaged three times with 0.4 ml of PBS via a tracheal cannula. BAL cell counts are quoted number/ml of recovered BAL fluid. BAL fluid was centrifuged (700 X g, 5 min, 4°C); cells were resuspended in 0.5 ml complete media (RPMI + 10% fetal calf serum [FCS], 2 mM L-glutamine, 100 U/ml penicillin/streptomycin). Cells were counted and pelleted onto glass slides by cytocentrifugation (5 ×10^4 cells/slide). Differential cell counts were performed on Wright-Giemsa–stained cytospins. Percentages of eosinophils, lymphocyte/mononuclear cells, neutrophils, and macrophages were determined from a total of 400 cells. To obtain absolute numbers of each leukocyte subtype, these percentages were multiplied by the total number of cells obtained in the lavage fluid.

To disaggregate the cells from the lung tissue, one finely chopped left lobe of lung was incubated at 37°C for 1 h in digest reagent (0.15 mg/ml collagenase type D, 25 μg/ml DNase type I) in complete RPMI media. The recovered cells were filtered through a 70-μm nylon sieve, washed twice, resuspended in 1ml complete media, and counted in a hemocytometer prior to cytocentrifugation; lung cell counts are quoted as total cell number/ml of this suspension. Differential cell counts were performed on Wright-Giemsa stained cytospins. To obtain absolute numbers of each leukocyte subtype, these percentages were multiplied by the total number of cells recovered. All differential counts were performed blind and in a randomized order at the end of the study by the same observer.

Adoptive transfer studies

In order to obtain alveolar macrophages for adoptive transfer studies, airways of naïve WT or IRF5^{-/-} mice were lavaged six times with 0.5 ml of ice cold PBS via a tracheal cannula. Alveolar macrophages comprised >97% of the retrieved population as assessed by cytospin preparation and flow cytometric analysis, respectively. Cells were stained with the vibrant blue system (life technologies) as per the manufacturers instructions, prior to transfer (200,000 cells/recipient in 100μL sterile PBS) and >70% of transferred cells could be recovered 24h later. Anti-IL-13 antibody was a gift from UCB® Celltech, UK; 10mg/kg was administered prior to transfer of AMs, intra-peritoneally at day -2 and -4, respectively. An isotype-matched antibody was used as a control.

Histology

Paraffin-embedded sections (4 μm) of lungs (apical lobe) were stained with hematoxylin/ eosin (H&E), periodic acid-Schiff (PAS) and Sirius Red. For assessment of inflammatory infiltrate, a semiquantitative scoring system was used to grade the size of lung infiltrates as previously described[31]. Briefly, a score of 5 signified a large (> 3 cells deep) widespread inflammatory infiltrate around the majority of vessels and bronchioles, and a score of 1 represented a small (≤ 2 cells deep) number of inflammatory foci. For mucus assessment, airways were categorized according to the abundance of PAS-positive goblet cells and assigned numerical scores (0, <5% goblet cells; 1, 5–25%; 2, 25–50%; 3, 50 –75%; 4, >75%). The sum of the airway scores from each lung was divided by the number of airways examined to obtain the histological goblet cell score (expressed as mucus score in arbitrary units; AU). All scoring and measurements were performed blinded by the same observer on medium airways measuring between 150 and 250 μm in diameter. Epithelial cell height and thickness of the airway smooth muscle layer around medium sized conducting airways were measured from paraffin sections. At least 6 measurements were made per airway with a minimum of 6 airways measured per section. Data presented are % thickening in comparison to PBS treated WT control.

Over-expression of IRF5

Selected groups received a first-generation replication-deficient adenovirus serotype 5 containing human IRF5 (AdIRF5, 0.5×10^9 viral pfu in PBS) or a control mock vector (AdC) 2 days prior to commencing instillation of either HDM or PBS.

Quantification of Chemokines and Immunoglobulins

Chemokine levels were measured in lung homogenates (cardiac lobe, 50mg/ml). Paired antibodies for murine Eotaxin-2 and IL-10 (R&D systems, Abingdon, UK), TNF-α, IL-1β, IL-6, IL-13 (ebiosciences) and IFN-γ (BD Biosciences) were used in standardized sandwich ELISAs according to the manufacturer's protocol. Paired antibodies for IgE, IgG1 and IgG2a (R&D systems) were used to measure serum and lung antibody levels.

Quantification of total collagen

Total collagen was measured in lung tissue (cardiac lobe) by biochemical assay (Sircol collagen assay, Biocolor, Belfast, UK) and normalized for tissue weight (50mg/ml).

Flow cytometric analysis

Disaggregated lung (left lobe) or BAL cells were either stained without stimulation or stained following stimulation with 500 ng/mL of ionomycin and 50 ng/mL of phorbol 2-myristate 13-acetate in the presence of brefeldin (BD Pharmingen) or HDM (50 μg/ml). Cells were washed and pre-incubated with serum or Fc Block (2.4G2) prior to surface staining with the following antibodies purchased from (clones in brackets): Biolegend, inc.; F4/80 (BM8), CD68 (FA-11), ICOS (C3984A), eBioscience, inc.; IL-13 (ebio13A), IL-17 (ebio17B7), GR-1 (RB6-8C5), CD11c (N418), CD45 (30-F11), CD11b (M1/70), IFN-γ (XMG1.2), lineage cocktail (17A2, RA3-6B2, M1/70, TER-119, RB6-8C5); eBiosciences; Ly6c (AL21), CD4 (RM4-5), Siglec-F (E50-2440), T1/ST2 (RMST2-33). Total macrophage

populations were identified by CD68 or F4/80 staining. Labeled cells were acquired on a BD fluorescence-activated cell sorting LSR Fortessa (BD Bioscience) and further analyzed by using FlowJo (Treestar). Intra-nuclear staining for IRF5 was carried out using a Rabbit polyclonal antibody to IRF5 (Abcam, catalogue# ab178899), or for detection of full length IRF5 in overexpression studies, a Rabbit polyclonal antibody to IRF5 (Abcam, catalogue# ab175317), followed by Alexa Fluor® 488 Goat Anti-Rabbit IgG antibody (life-technologies). Surface staining was followed by fixation and then permeabilisation to allow for intracellular or intra-nuclear staining.

Real-time PCR

Total RNA was extracted from 50 to 100 mg of lung tissue (azygous lobe) using a Qiagen RNeasy Mini Kit. Total RNA (1 μg) was reverse transcribed into cDNA using a High Capacity cDNA Reverse Transcription Kit (Life Technologies) as per the manufacturer's instructions. Real-time PCR reactions were performed using fast-qPCR mastermix (Life technologies) on a Viaa-7 instrument (Life Technologies) with TaqMan primer sets for murine IL-4, IL-5, IL-13, eotaxin-2, fibronectin, collagen-1α1, Mucin 5B, Mucin 5ac, Arg-1, YM-1, iNOs, TGF-β1, TGF-β2, TGF-β3, GAPDH or HPRT (Life Technologies) and gene expression was analyzed using the change-in-threshold ΔΔCt-method, fold-changes in mRNA expressions for targeted genes were calculated relative to wild-type controls.

Statistical analysis

Data were analyzed using Prism 6 for Windows from GraphPad Software Inc, using Kruskal-Wallis or Mann-Whitney tests.

Supplementary Materials

Refer to Web version on PubMed Central for supplementary material.

Acknowledgements

References

1. Chanez P, et al. Severe asthma in adults: What are the important questions? Journal of Allergy and Clinical Immunology. 2007; 119:1337–1348. [PubMed: 17416409]

2. Anderson GP. Interactions between corticosteroids and beta-adrenergic agonists in asthma disease induction, progression, and exacerbation. Am J Respir Crit Care Med. 2000; 161:S188–96. [PubMed: 10712373]

3. Krausgruber T, et al. IRF5 is required for late-phase TNF secretion by human dendritic cells. Blood. 2010; 115:4421–4430. [PubMed: 20237317]

4. Krausgruber T, et al. IRF5 promotes inflammatory macrophage polarization and T. Nature Immunology. 2011; 12:231–238. [PubMed: 21240265]

5. Ryzhakov G, Eames HL, Udalova IA. Activation and Function of Interferon Regulatory Factor 5. Journal of Interferon & Cytokine Research. 2014; 140926135928001. doi: 10.1089/jir.2014.0023

6. Lee YH, Bae S-C, Choi SJ, Ji JD, Song GG. Associations between interferon regulatory factor 5 polymorphisms and rheumatoid arthritis: a meta-analysis. Mol Biol Rep. 2012; 40:1791–1799. [PubMed: 23073787]

7. Lessard CJ, et al. Variants at multiple loci implicated in both innate and adaptive immune responses are associated with Sjögren's syndrome. Nat Genet. 2013; 45:1284–1292. [PubMed: 24097067]

8. Salloum R, Niewold TB. Interferon regulatory factors in human lupus pathogenesis. Translational Research. 2011; 157:326–331. [PubMed: 21575916]

9. Gathungu G, Zhang CK, Zhang W, Cho JH. A two-marker haplotype in the IRF5 gene is associated with inflammatory bowel disease in a North American cohort. Genes and Immunity. 2012; 13:351–355. [PubMed: 22257839]

10. Wang C, et al. Evidence of association between interferon regulatory factor 5 gene polymorphisms and asthma. Gene. 2012; 504:220–225. [PubMed: 22613848]

11. Dobbs LG, Johnson MD. Alveolar epithelial transport in the adult lung. Respiratory Physiology & Neurobiology. 2007; 159:283–300.

12. Byrne AJ, Mathie SA, Gregory LG, Lloyd CM. Pulmonary macrophages: key players in the innate defence of the airways. Thorax. 2015; 70:1189–1196. [PubMed: 26286722]

13. Hussell T, Bell TJ. Alveolar macrophages: plasticity in a tissue-specific context. Nature Reviews Immunology. 2014; 14:81–93. [PubMed: 24445666]

14. Mathie SA, et al. Alveolar macrophages are sentinels of murine pulmonary homeostasis following inhaled antigen challenge. Allergy. 2015; 70:80–89. [PubMed: 25331546]

15. Bedoret D, et al. Lung interstitial macrophages alter dendritic cell functions to prevent airway allergy in mice. J Clin Invest. 2009; 119:3723–3738. [PubMed: 19907079]

16. Kim HY, et al. Interleukin-17–producing innate lymphoid cells and the NLRP3 inflammasome facilitate obesity-associated airway hyperreactivity. Nat Med. 2013; 20:54–61. [PubMed: 24336249]

17. Fang C-M. Unique contribution of IRF-5-Ikaros axis to the B-cell IgG2a response. 2012; 13:421–430.

18. Feng D, et al. Irf5-deficient mice are protected from pristane-induced lupus via increased Th2 cytokines and altered IgG class switching. Eur J Immunol. 2012; 42:1477–1487. [PubMed: 22678902]

19. Roy MG, et al. Muc5b is required for airway defence. Nature. 2013; 505:412–416. [PubMed: 24317696]

20. Zsengellér Z, Otake K, Hossain SA, Berclaz PY, Trapnell BC. Internalization of adenovirus by alveolar macrophages initiates early proinflammatory signaling during acute respiratory tract infection. Journal of Virology. 2000; 74:9655–9667. [PubMed: 11000238]

21. Kim EY, et al. Persistent activation of an innate immune response translates respiratory viral infection into chronic lung disease. Nat Med. 2008; 14:633–640. [PubMed: 18488036]

22. Wills-Karp M. Interleukin-13: Central mediator of allergic asthma. Science. 1998; 282:2258–2261. [PubMed: 9856949]

23. Hancock A, Armstrong L, Gama R, Millar A. Production of Interleukin 13 by alveolar macrophages from normal and fibrotic Lung. Am J Respir Cell Mol Biol. 2012; 18:60–65.

24. Grünig G, et al. Requirement for IL-13 independently of IL-4 in experimental asthma. Science. 1998; 282:2261–2263. [PubMed: 9856950]

25. Shirey KA, et al. Control of RSV-induced lung injury by alternatively activated macrophages is IL-4R. Mucosal Immunology. 2010; 3:291–300. [PubMed: 20404812]

26. Kang C-M, et al. Interleukin-25 and Interleukin-13 Production by Alveolar Macrophages in Response to Particles. Am J Respir Cell Mol Biol. 2005; 33:290–296. [PubMed: 15961726]

27. Yang Z, et al. Macrophages as IL-25/IL-33-responsive cells play an important role in the induction of type 2 immunity. PLoS ONE. 2013; 8:e59441–e59441. [PubMed: 23536877]

28. Tourdot S, et al. Respiratory syncytial virus infection provokes airway remodelling in allergen-exposed mice in absence of prior allergen sensitization. Clin Exp Allergy. 2008; 38:1016–1024. [PubMed: 18498543]

29. Anthony D, et al. SAA drives proinflammatory heterotypic macrophage differentiation in the lung via CSF-1R-dependent signaling. The FASEB Journal. 2014; 28:3867–3877. [PubMed: 24846388]

30. Stouch AN, et al. I B Kinase activity drives fetal lung macrophage maturation along a non-M1/M2 Paradigm. J Immunol. 2014; 193:1184–1193. [PubMed: 24981452]

31. Saglani S, et al. Pathophysiological Features of Asthma Develop in Parallel in House Dust Mite–Exposed Neonatal Mice. Am J Respir Cell Mol Biol. 2009; 41:281–289. [PubMed: 19151316]

32. Saigusa R, et al. Multifaceted contribution of the TLR4-activated IRF5 transcription factor in systemic sclerosis. PNAS. 2015; 112(49):15136–41. [PubMed: 26598674]

33. Dalmas E, et al. Irf5 deficiency in macrophages promotes beneficial adipose tissue expansion and insulin sensitivity during obesity. Nat Med. 2015; 21(6):610–8. [PubMed: 25939064]
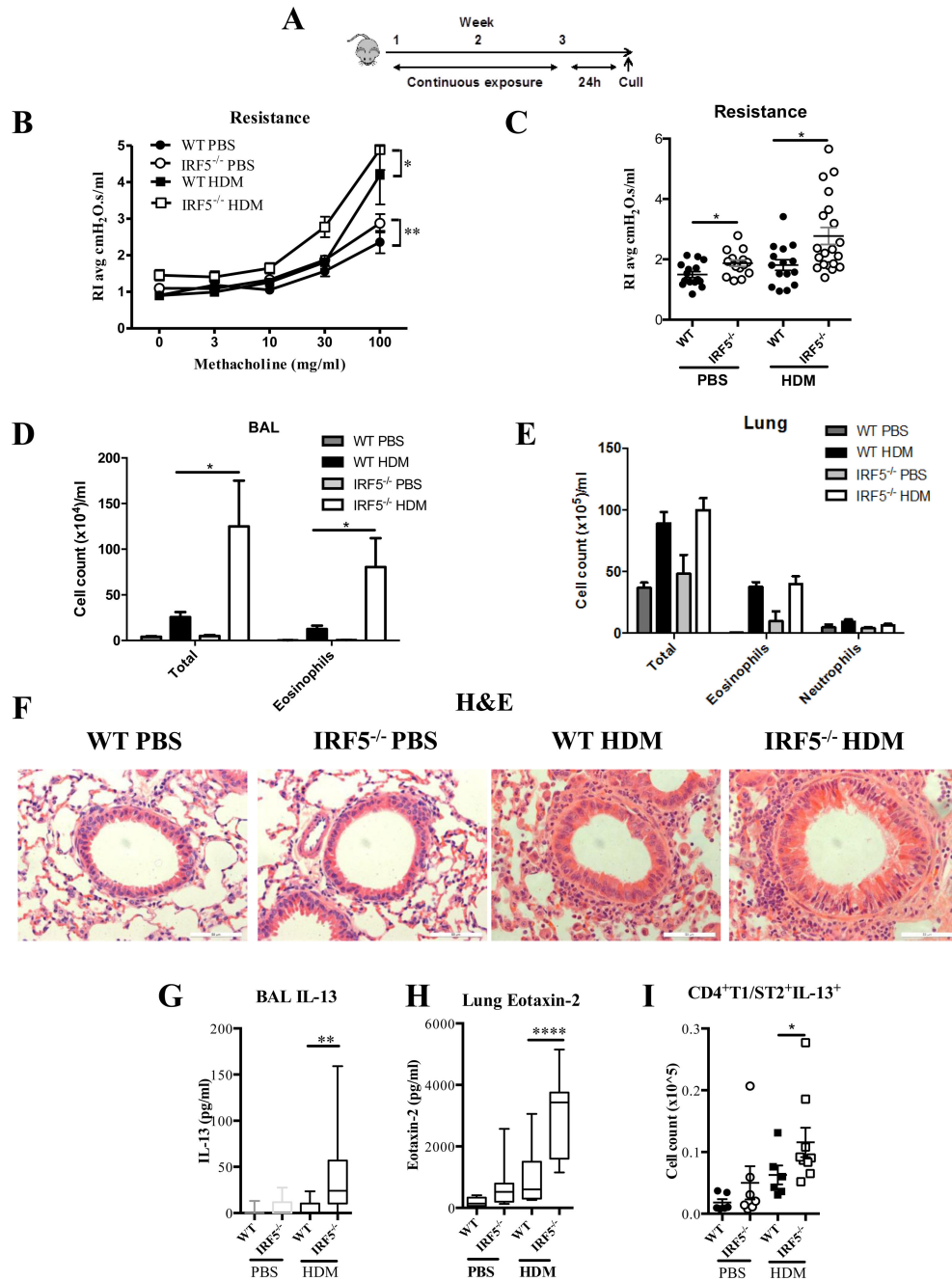
Figure 1. IRF5 is a critical component of pulmonary homeostasis and Type 2 responses after HDM exposure.

(**A**) Experimental design of HDM-induced allergic airways disease. Resistance measured in tracheotomised animals to a dose response (**B**) or at a representative dose of 30 mg/ml of methacholine (**C**). Differential cell counts of Wright-Giemsa stained cytospins recovered from the BAL (**D**) and lung (**E**). (**F**) Lung sections stained with H&E; original magnification x40; Scale bar = 50 μm, representative photomicrographs are shown. IL-13 levels in the BAL (**G**) and Lung eotaxin-2 (**H**) and as determined by ELISA. (**I**) CD4+T1/ST2+IL-13+ Th2 cells recovered from the lung and quantified by flow cytometry. Data shown represent

means ± standard error mean (s.e.m.), *P < 0.05, **P < 0.01, ****P < 0.0001 WT compared with IRF5$^{-/-}$ animals by Mann-Whitney test. Data were generated from four independent experiments; *n*=7-20 per group.
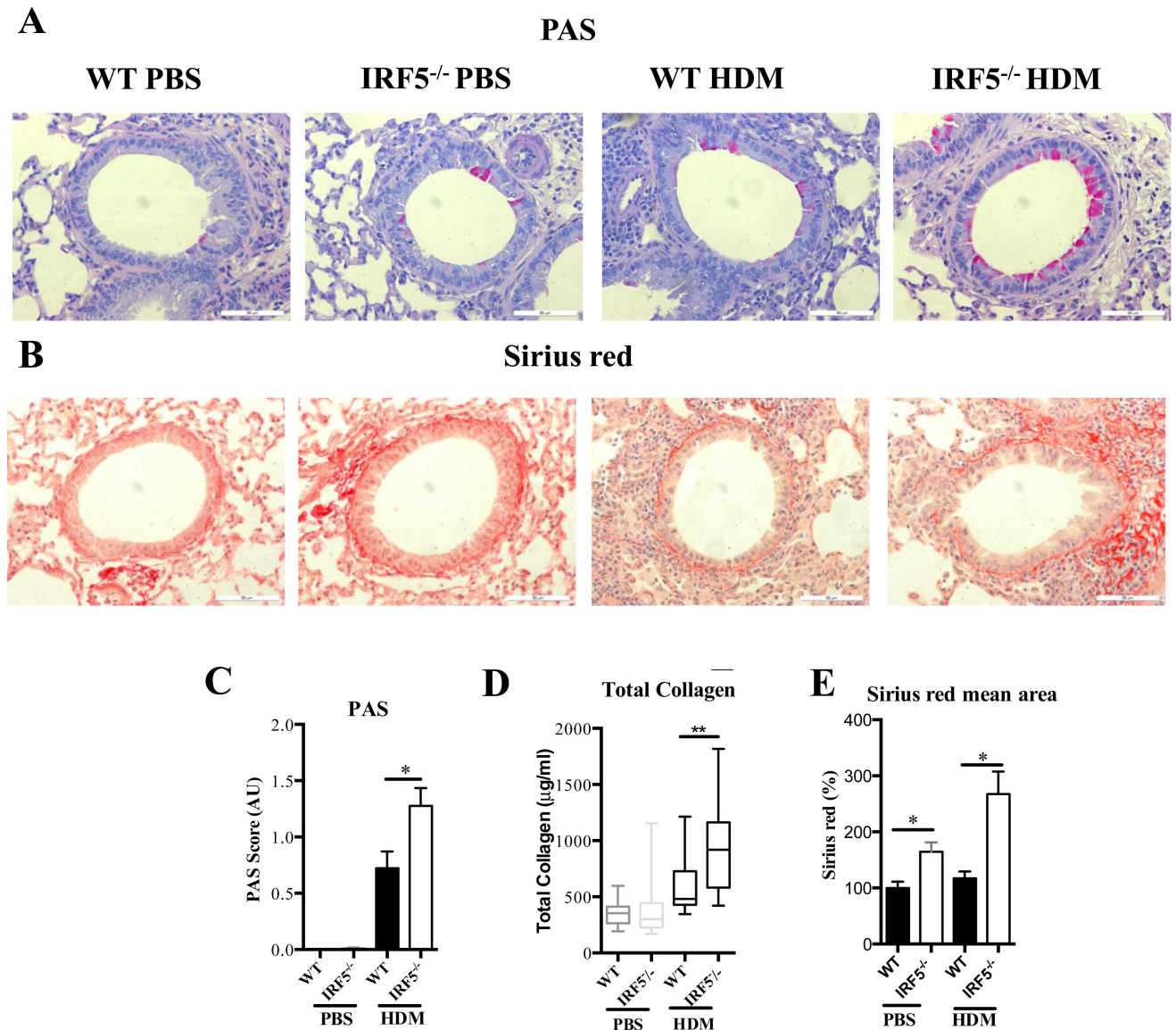
Figure 2. IRF5 deficiency leads to augmented mucus and collagen production in the lung after HDM exposure.

Lung sections stained with PAS (**A**) and Sirius red (**B**), respectively. PAS staining to identify mucin-containing cells (purple, top panel); Sirius Red staining of lung sections depicts peri-bronchiolar and perivascular collagen (red, bottom panel), original magnification x40; Scale bar = 50 μm, representative photomicrographs are shown. (**C**) Scoring of lung sections stained with periodic acid-Schiff. (**D**) Recently synthesized total lung collagen was quantified by a biochemical (Sircol) assay. (**E**) Quantitative image analysis of sub-epithelial peri-bronchiolar collagen density determined by measuring Sirius red-stained collagen in lung sections under polarized light; data was normalized to WT untreated control and expressed as percent (%) increase. Data shown represent means ± standard error mean (s.e.m.), *P < 0.05, **P < 0.01, WT compared with IRF5$^{-/-}$ animals by Mann-Whitney test.

Box and whisker plots represent the mean, IQR and minimum and maximum values. Data were generated from four independent experiments; *n*=15–20 per group.
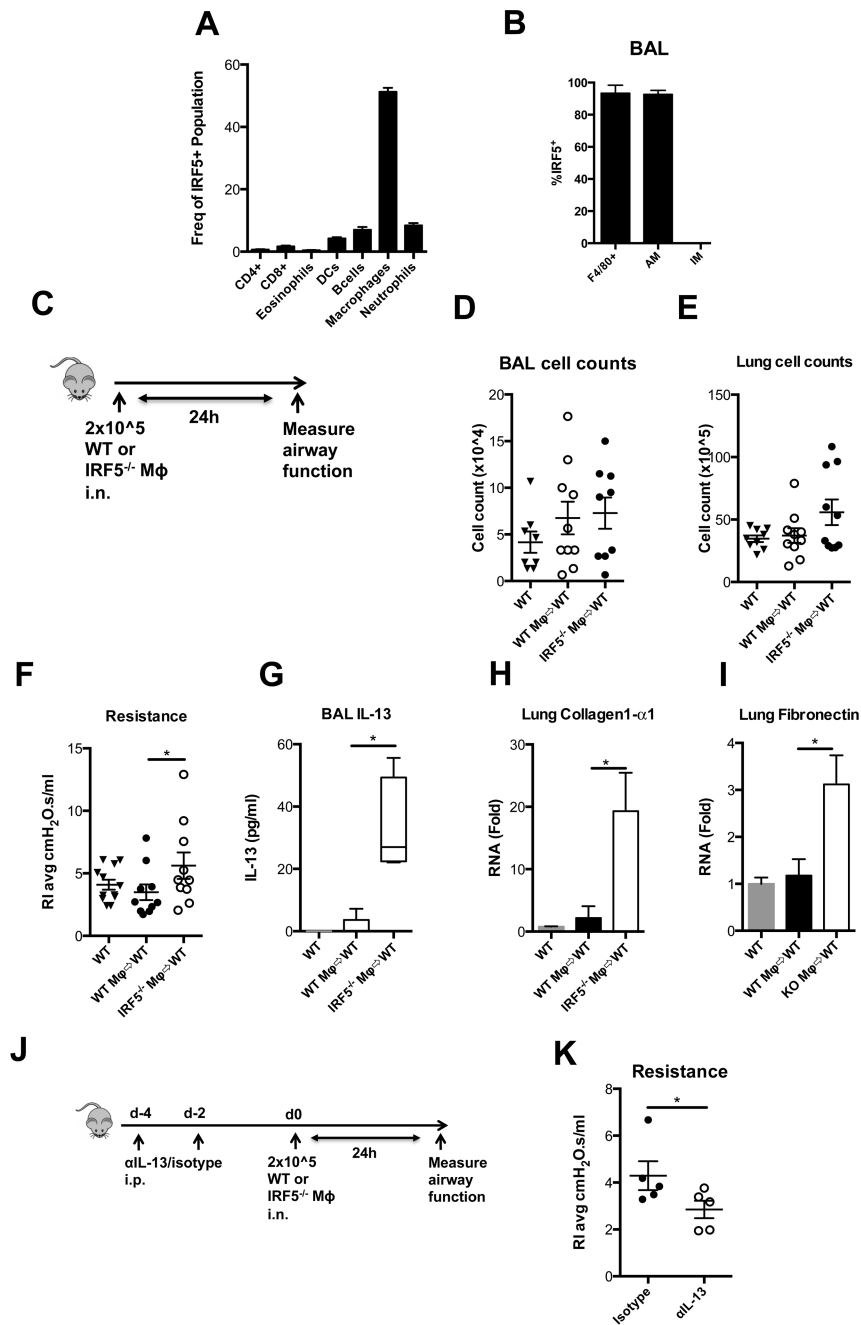
Figure 3. IRF5 deficient macrophages are pro-fibrotic.
(**A**) Flow cytometric analysis of lung F4/80 positive cells recovered from whole lung homogenates, without BAL. (**B**) Flow cytometric analysis of lung F4/80 positive cells recovered from BAL. (**C**) Schematic for adoptive transfer model. Total counts of cells recovered from the BAL (**D**) and lung (**E**). (**F**) Resistance measured in tracheotomised animals at a 300 mg/ml dose of methacholine. (**G**) BAL IL-13 levels as determined by ELISA. Expression of collagen-1α1 (**H**) and (**I**) fibronectin after methacholine challenge in whole lung homogenates as measured by qPCR, fold changes are calculated relative to naïve

wild-type controls. (**J**) Dosing regimen and experimental design for IL-13 blocking experiment. (**K**) Resistance measured in tracheotomised animals at a 300 mg/ml dose of methacholine. Data shown represent mean ± s.e.m. *P < 0.05, WT compared with IRF5^{-/-} animals by Mann-Whitney test. Box and whisker plots represent the mean, IQR and minimum and maximum values. Data were generated from two independent experiments; *n*=4-10 per group.
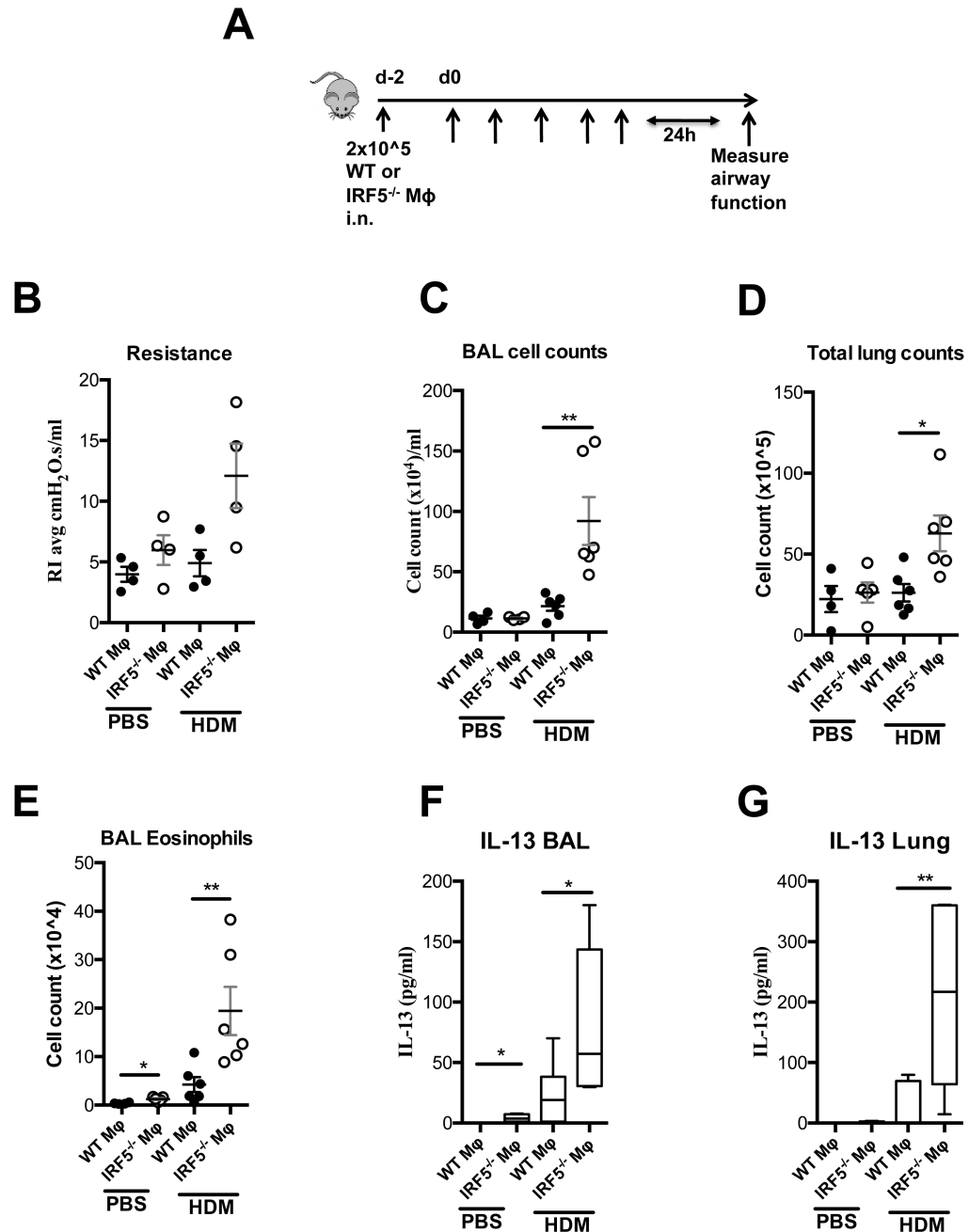
Figure 4. IRF5-expressing AMs control responses to inhaled aeroallegen
A) Schematic for adoptive transfer model. (**B**) Resistance measured in tracheotomised animals at a 300 mg/ml dose of methacholine. Total counts of cells recovered from the BAL (**C**) and lung (**D**). Total numbers of eosinophils recovered from the BAL (**E**) and IL-13 producing innate lymphoid cells recovered from the lung (**F**). BAL (**G**) and lung (**H**) IL-13 levels as determined by ELISA. Data shown represent mean ± s.e.m. *P < 0.05, WT compared with IRF5^{-/-} animals by Mann-Whitney test. Box and whisker plots represent the mean, IQR and minimum and maximum values; *n*=4-6 per group.
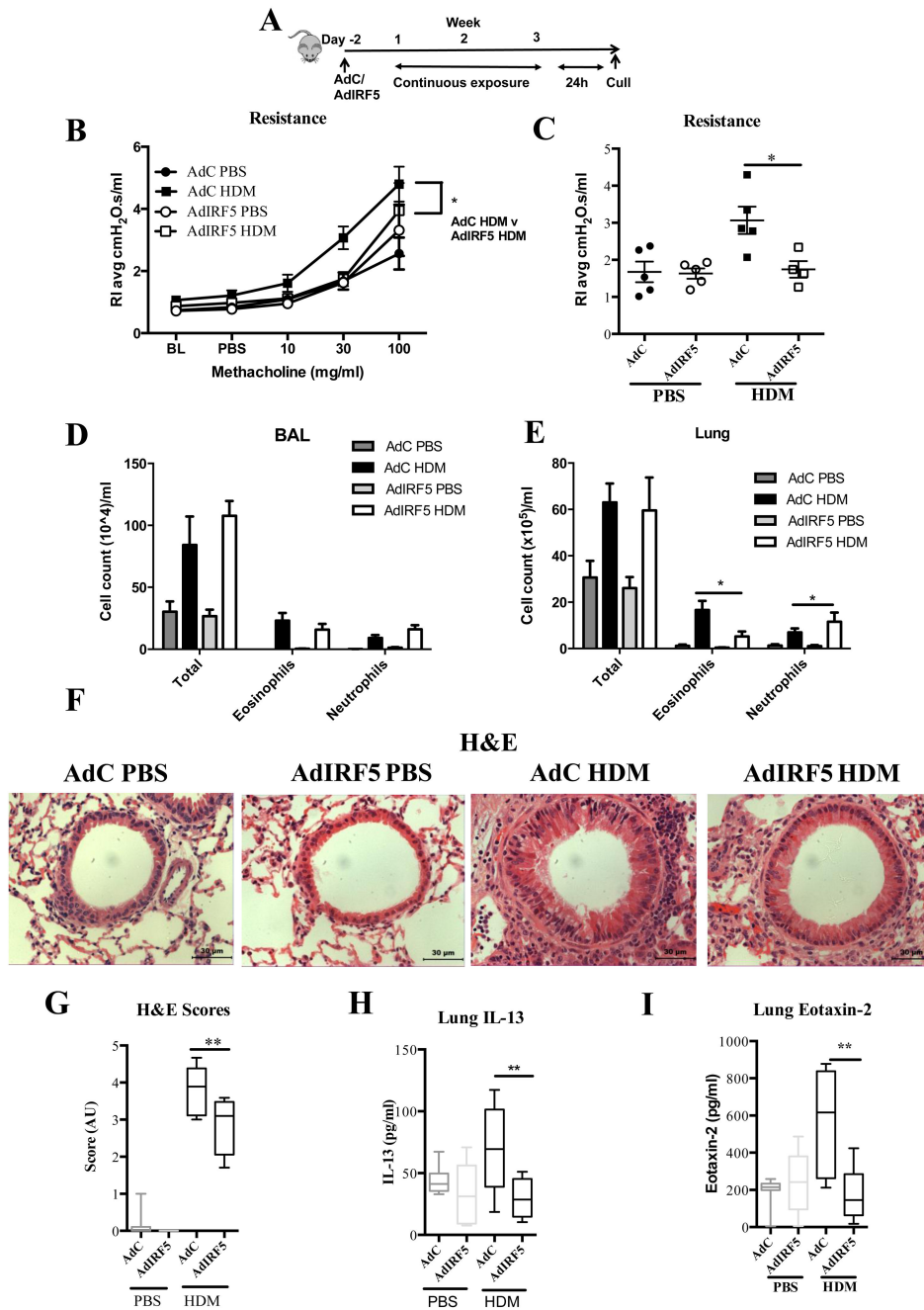
Figure 5. Overexpression of IRF5 ameliorates house dust mite-mediated airway hyper-responsiveness and inflammation.

(**A**) Experimental design of HDM-induced allergic airways disease. Resistance measured in tracheotomised animals to a dose response (**B**) or at a representative dose of 30 mg/ml of methacholine (**C**); *n*=4-5 per group. Differential cell counts of Wright-Giemsa stained cytospins recovered from the BAL (**D**) and lung (**E**); *n*=4-5 per group. (**F**) Lung sections stained with H&E; original magnification x40; Scale bar = 50 μm, representative photomicrographs are shown. (**G**) Semi-quantitative scoring of H&E (i) sections. Lung IL-13 (**H**) and eotaxin-2 (**I**) levels and as determined by ELISA. Data shown represent

means ± standard error mean (s.e.m.), *P < 0.05, **P < 0.01, WT compared with IRF5^{-/-} animals by Mann-Whitney test. Box and whisker plots represent the mean, IQR and minimum and maximum values. Data were generated from three independent experiments; *n*=10-15 per group.
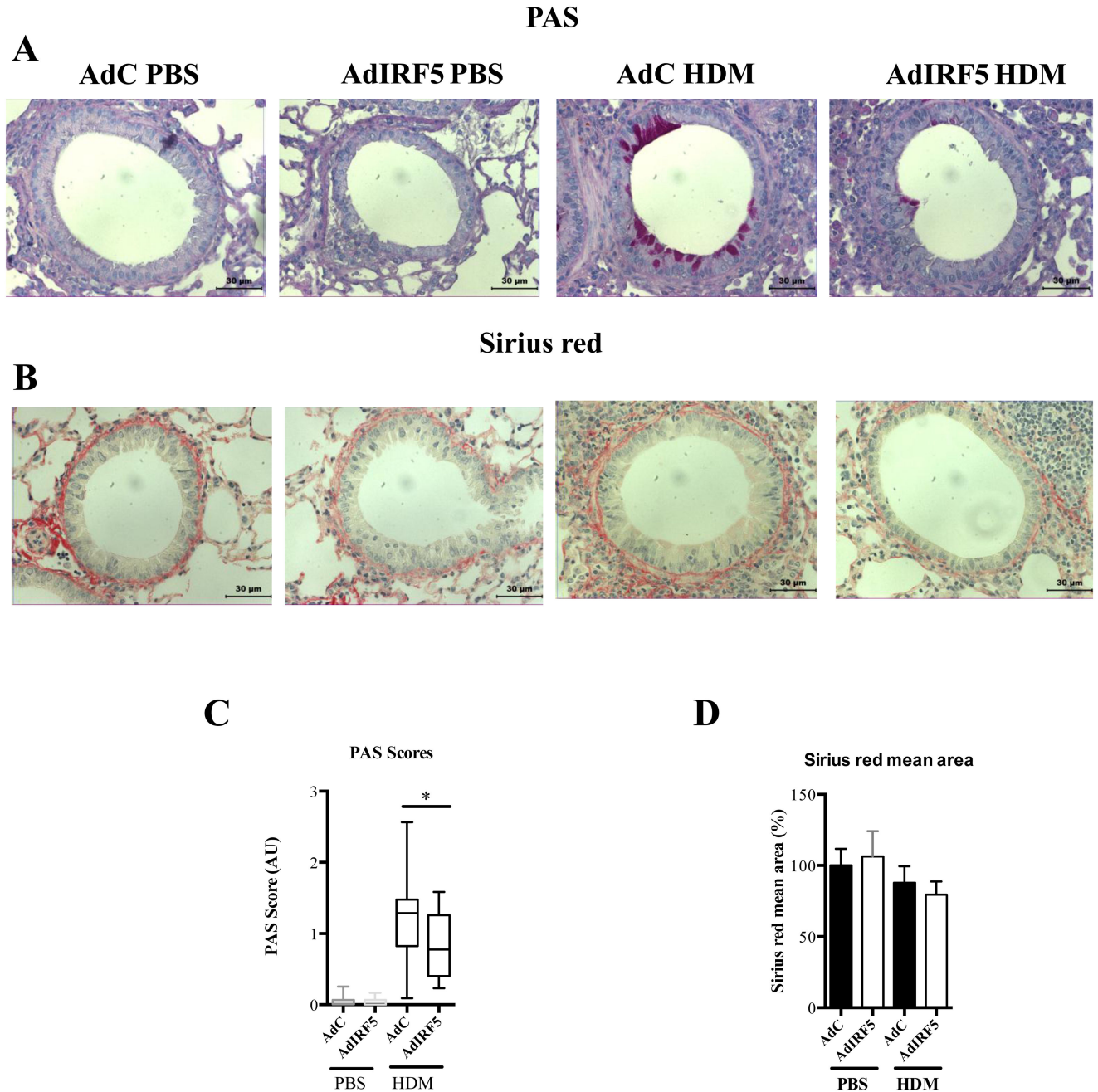
PAS

A

| AdC PBS | AdIRF5 PBS | AdC HDM | AdIRF5 HDM |

Sirius red

B

C

PAS Scores

D

Sirius red mean area

Figure 6. Overexpression of IRF5 deficiency leads to reduced mucus production in the lung after HDM exposure.

Lung sections stained with PAS (**A**) and Sirius red (**B**), respectively. PAS staining to identify mucin-containing cells (purple, top panel); Sirius Red staining of lung sections depicts peri-bronchiolar and perivascular collagen (red, bottom panel), original magnification x40; Scale bar = 50 μm, representative photomicrographs are shown. (**C**) Scoring of lung sections stained with periodic acid-Schiff. (**D**) Quantitative image analysis of sub-epithelial peri-bronchiolar collagen density determined by measuring Sirius red-stained collagen in lung sections under polarized light; data was normalized to AdC PBS control and expressed as

percent (%) increase. Data shown represent means ± s.e.m. from two individual experiments *P < 0.05, WT compared with IRF5^{-/-} animals by Mann-Whitney test. Box and whisker plots represent the mean, IQR and minimum and maximum values. Data were generated from three independent experiments; n=10-15 per group.